Journal of ELECTRONIC MATERIALS, Vol. 45, No. 9, 2016
DOI: 10.1007/s11664-016-4659-2
© 2016 The Minerals, Metals & Materials Society

CrossMark

Dynamics of Kinetically Limited Strain and Threading Dislocations in Temperature- and Compositionally Graded ZnSSe/GaAs (001) Metamorphic Heterostructures

TEDI KUJOFSA[1,2] and J.E. AYERS[1]

1.—Electrical and Computer Engineering Department, University of Connecticut, 371 Fairfield Way, Unit 4157, Storrs, CT 06269-4157, USA. 2.—e-mail: Tedi.Kujofsa@gmail.com

We have investigated the evolution of the strain and threading dislocation density in metamorphic compositionally and temperature-graded ZnS_ySe_{1-y} buffer layers. Linear variation in composition in conjunction with temperature grading may allow control over the relaxation process. Previously, we reported the development of a general kinetic model based on dislocation flow, which accounted for the time evolution of the strain relaxation in semiconductor structures under kinetically limited conditions, including interactions of threading and misfit defects. In this work, we studied ZnS_ySe_{1-y}/GaAs (001) heterostructures with linear compositional grading and a convex-upward (type A), linear (type B) or convex-downward (type C) temperature grading profile. The thermal budget available for relaxation in these types of structures is controlled by the temperature grading profile, made up of combinations of linear ramps and constant-temperature sections. In all cases, the temperature was varied from T_0 (400°C to 600°C) at the substrate interface to T_F = 300°C at the surface. We also investigated the effect of varying the compositional gradient in the range from 0.18%/μm to 1.6%/μm. Structures with higher average temperature (greater thermal budget) and/or higher grading coefficient exhibited greater extent of relaxation and therefore reduced residual strain. Furthermore, controlling the extent of strain relaxation enabled optimization of the dislocation densities in these heterostructures.

Key words: Relaxation, strain, temperature- and compositionally graded buffer, threading dislocations, ZnSSe/GaAs

INTRODUCTION

The design of highly functional and reliable microelectronic and optical devices requires use of metamorphic buffer layers (MBLs) to accommodate misfit strain associated with growth of lattice-mismatched materials. However, such metamorphic growth generates dislocation defects that are detrimental to device performance, so novel approaches are required to control the extent of strain relaxation and dislocation generation.

Metamorphic device heterostructures employ a wide range of compositional profiles, including linearly graded,[1–4] step graded,[5–7] or nonlinear and continuously graded buffer layers.[8–11] The main benefit of compositionally graded epitaxial layers is that they enable distribution of misfit dislocations throughout the graded layer, in turn reducing any dislocation pinning interactions with substrate-associated defects or material that may be grown on top of the MBL. In addition, use of a compositionally graded layer promotes growth of misfit dislocation length, in turn resulting in lower density of threading dislocations emanating from misfit segments.[1,2,9–11] A consequential benefit of compositionally graded MBL is that the surface misfit dislocation-free zone provides high built-in strain which could aid in sweeping threading

(Received November 11, 2015; accepted May 12, 2016; published online June 21, 2016)

dislocation arms.[9–11] In addition, several studies have shown that growth at reduced temperature can decrease surface roughness[12–16] and material quality,[17–19] yielding devices with improved threading dislocation density.

In a previous paper,[20] we reported use of a temperature grading scheme and studied the lattice relaxation and threading dislocations in uniform layers of ZnSe grown on GaAs (001). In the growth of a compositionally uniform layer, all misfit dislocations are located at the interface, and the only means for reducing the threading density are promotion of longer misfit segments or growth of relatively thick layers, to enhance annihilation and coalescence reactions between defects. In the previous work with uniform layers, we showed that, by employing a temperature grading scheme and thereby controlling the thermal budget available for relaxation, we could optimize the relaxation process as well as the dislocation density by enhancing thermally activated glide. However, the mismatch constraints imposed by the ZnSe/GaAs material system enabled us to use compositionally graded ZnSSe/GaAs (001) buffer layers in conjunction with temperature grading to allow greater flexibility in the design of mismatched heterostructures.

In this work, we applied a generalized kinetic model for strain relaxation and dislocation dynamics to investigate the combined effect of temperature and compositional grading on the lattice relaxation mechanism in ZnSSe/GaAs heterostructures. In this model, it is assumed that the dislocation multiplication rate is proportional to the glide velocity, the effective stress, and the defect density; this is based on the model proposed by Dodson and Tsao[21,22] but includes the time variation of the equilibrium strain and temperature during growth and is therefore applicable to graded materials. In addition, we accounted for dislocation–dislocation interactions, including the following two mechanisms: (i) dislocation compensation caused by interactions of misfit–threading dislocations at abrupt interfaces; and (ii) annihilation and coalescence reactions as described by Tachikawa et al.[23] Here, we extended the previous work[20] by utilizing three different temperature grading profiles in conjunction with linear compositional variation to study the evolution of kinetically limited lattice relaxation and threading dislocation behavior. In addition, we examined the combined effect of the available thermal budget and the grading constant on the lattice relaxation process.

EQUILIBRIUM, KINETICALLY LIMITED LATTICE RELAXATION AND DISLOCATION DYNAMICS MODELS

In this work, we considered heterostructures involving a linearly graded ZnS_ySe_{1-y} layer grown on top of a GaAs (001) substrate. The lattice mismatch is defined as $f(z) \equiv [a_s - a(z)]/a(z)$, where a_s is the relaxed lattice constant of the substrate and $a(z)$ is the relaxed lattice constant of the epitaxial crystal at distance z from the substrate interface. For linearly graded metamorphic buffer layers, the lattice mismatch profile at distance z from the substrate interface is given by

$$f(z) = C_f z, \quad (1)$$

where C_f is the grading constant. The equilibrium configuration may be determined numerically by minimizing the sum of the strain and dislocation energies, using an approach similar to that described by Bertoli et al.[24] Equilibrium calculations serve as the starting point for determination of kinetically limited lattice relaxation. The foundation for the kinetically limited lattice relaxation and dislocation dynamics model along with the material/model parameters used in this work are explained in more detail in Refs. 25 and 26, respectively. The kinetic model predicts the lattice relaxation and dislocation behavior in (001) arbitrary heteroepitaxial layers, which may incorporate graded and multilayered structures. The main assumptions of the model are that, at distance z from the substrate interface: (i) the lattice relaxation rate is governed by the glide of all the misfit dislocations concentrated below, and (ii) the glide of the dislocations is governed by the glide force acting on the threading arms of dislocations concentrated above. Furthermore, we developed a dislocation dynamics model to study threading and misfit dislocation behavior. We included two important misfit–threading dislocation interactions, namely: (i) introduction of dislocation half-loops,[27] and (ii) bending over of existing threading dislocations at mismatched interfaces.[28] In addition, there may be second-order coalescence and annihilation reactions involving threading dislocations, as modeled by Romanov et al.[29] and Tachikawa et al.[23]

RESULTS AND DISCUSSION

In this work, we considered heterostructures utilizing a combination of temperature grading and linear compositional variation to explore the dependence of the in-plane strain and threading dislocations. Figure 1 shows the growth temperature versus accumulated thickness for each type of temperature grading profile. Sample type A (convex-upward profile) involves constant-temperature growth followed by a linear ramp from T_0 to T_F. Sample type B incorporates only a linear ramp from T_0 to T_F. Sample type C (convex-downward profile) incorporates a linear ramp from T_0 to T_F followed by constant-temperature growth. Furthermore, the lattice mismatch profile for the structures considered in this work employed a linear compositional grading scheme (as shown in Fig. 1), whereby the epilayer is graded from lattice matched at the substrate interface (y_0 = 6%, f_0 = 0%) to an ending mismatch (y_h, f_h), where y_0 is the sulfur mole

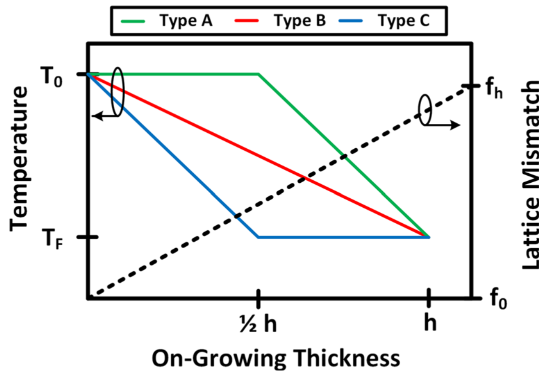

Fig. 1. Temperature (left axis) as a function of grown thickness for type A, B, and C structures. T_0 and T_F correspond to the temperature at the substrate interface and surface (h), respectively. Lattice mismatch profile (right axis) as a function of grown thickness. f_0 and f_h correspond to the lattice mismatch at the substrate interface and surface, respectively.

fraction. Here, we consider structures with epilayer thickness of 1 μm and ending sulfur mole fraction y_h ranging from 10% to 40%, corresponding to lattice mismatch of 0.18% to 1.58%, respectively. In thermodynamic terms, for given grading constant, the available thermal budget during growth is highest in structures utilizing the convex-upward temperature profile (type A), whereas it is lowest for convex-downward temperature grading (type C). In the simplest sense, the thermal budget refers to the average temperature multiplied by the growth time. However, many processes—including glide of dislocations—are thermally activated, making it more appropriate to consider the mean value of $\exp(-U/k_BT)$. In the cases studied herein, samples with higher average temperature also had higher average value of $\exp(-U/k_BT)$, and these can be referred to as having greater thermal budget than samples with lower average temperature and also lower average value of the exponent.

Figure 2 contrasts the evolution of the average in-plane strain, lattice mismatch, and equilibrium strain for the three types of samples, with initial growth temperature of 400°C. The structures considered here have 40% sulfur ending composition, corresponding to lattice mismatch of 1.58%. Whereas the equilibrium model shows a rapid relaxation process, especially in the early stages of growth, kinetically limited lattice relaxation in ZnS_ySe_{1-y} epitaxial layers predicts a much more gradual behavior exhibiting four distinct regimes (pseudomorphic, sluggish, rapid, and saturation). Although the onset of lattice relaxation in equilibrium occurs at approximately ~180 nm, depending on the temperature profile, it is apparent that the onset of kinetically limited lattice relaxation could occur from 400 nm to 500 nm. The results also indicate that the design of the temperature grading profile and therefore the thermal budget available for lattice relaxation may alter the relaxation

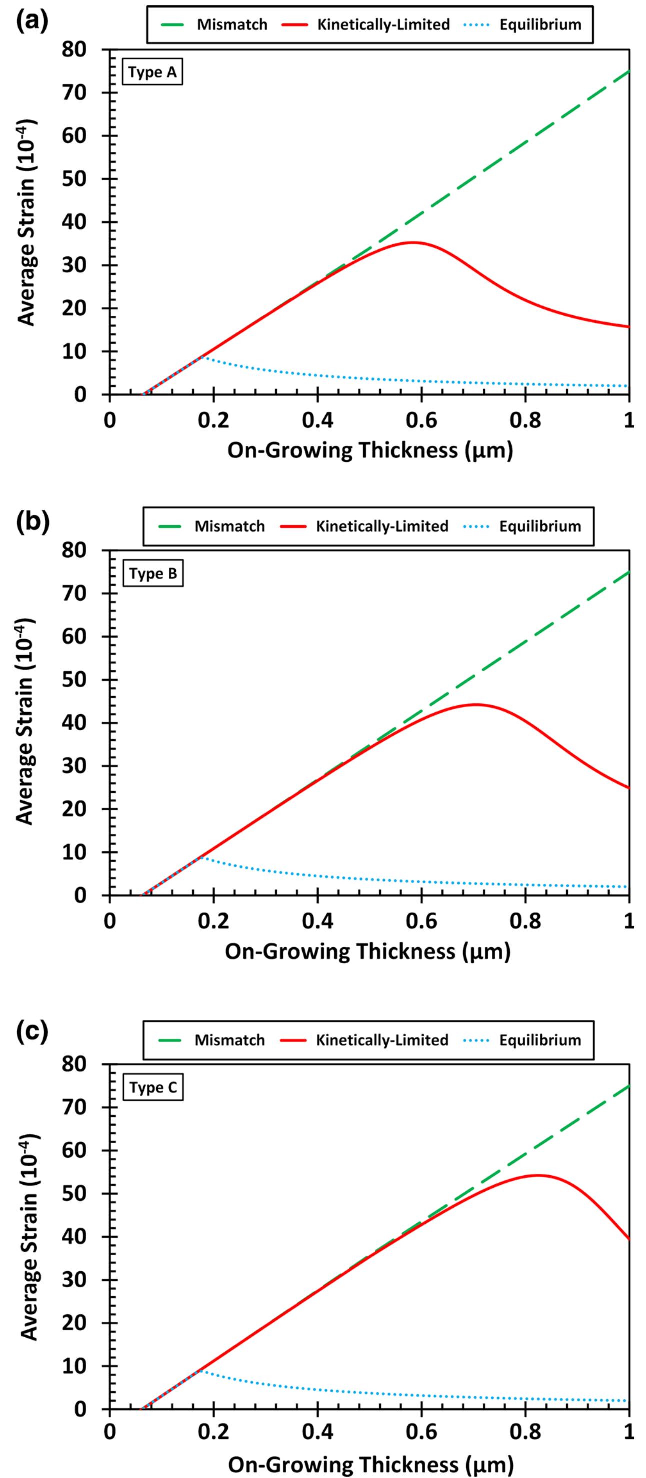

Fig. 2. Evolution of average strain (kinetically limited, mismatch, and equilibrium) as function of on-growing thickness for type (a) A, (b) B, and (c) C structures. The initial T_0 and final T_F temperatures in these structures are 400°C and 300°C, respectively. The ending sulfur composition is fixed at 40% (f_h = 1.58%).

kinetics in such a way that four-regime behavior is no longer clearly visible. The results in Fig. 2a–c show that the sluggish lattice relaxation regime is

more evident in structures with lower thermal budget (type C), whereas in type A structures, higher thermally activated glide velocities yield a faster lattice relaxation process. Regardless of the temperature grading profile, a minimum thermal budget is required to ensure onset of lattice relaxation. Furthermore, there also exists a critical thermal budget for attainment of near-complete relaxation. As an example, use of a convex-downward temperature grading profile could result in sluggish relaxation rates which yield structures with an in-plane strain value comparable to the lattice mismatch (about ~50% average relaxation in this case) even for a 1-μm-thick epitaxial layer. However, the strain relaxation in structures with a convex-upwards temperature profile at the given thickness approaches the equilibrium in-plane strain with a near-complete value of 85% average relaxation.

Figure 3 presents the average in-plane strain as a function of the compositional grading coefficient with initial growth temperature as a parameter for type A (Fig. 3a), B (Fig. 3b), and C (Fig. 3c) structures. For the cases considered here, the starting growth temperature was in the range from 400°C to 600°C in 50°C steps. The ending temperature was fixed at T_F = 300°C. In addition, the grading constant ranged from 0.18%/μm to 1.58%/μm. The results in Fig. 3a–c are similar in character to those in Fig. 2. The results in Fig. 3a–c indicate that a critical grading constant is required to enable onset of lattice relaxation. This critical grading constant strongly depends on the available thermal budget and therefore the temperature grading profile along with its initial and ending conditions. The average in-plane strain exhibits two-regime behavior. In the first regime, the average in-plane strain increases monotonically with increasing grading constant, whereas in the second regime, the average in-plane strain decreases with increasing grading constant. The first regime corresponds to the initial stages (pseudomorphic and sluggish) of lattice relaxation, while the second regime is correlated with the later stages of lattice relaxation (rapid and saturation). The results in Fig. 3a–c indicate that higher thermal budget results in faster onset of lattice relaxation. For type A structures, the critical grading constant is approximately 0.5%/μm, whereas for type B and C structures, the critical grading constant is 0.6%/μm and 1%/μm, respectively. Furthermore, increasing the initial growth temperature in these structures results in a lower grading constant for commencement of lattice relaxation. In addition, use of higher thermal budget results in diminishment of the region with approximately constant strain, as evident from the faster transition from the increasing to decreasing strain regimes as a function of increasing grading constant. The use of the convex-upwards temperature grading profile provides a greater thermal budget and therefore enhances the strain relaxation process, resulting in near-completely relaxed structures at relatively low grading constant; For example, at initial temperature T_0 = 600°C, the type A temperature grading profile yields 85% strain relaxation at grading constant $C_f \approx 1\%/\mu$m, whereas for type B and C

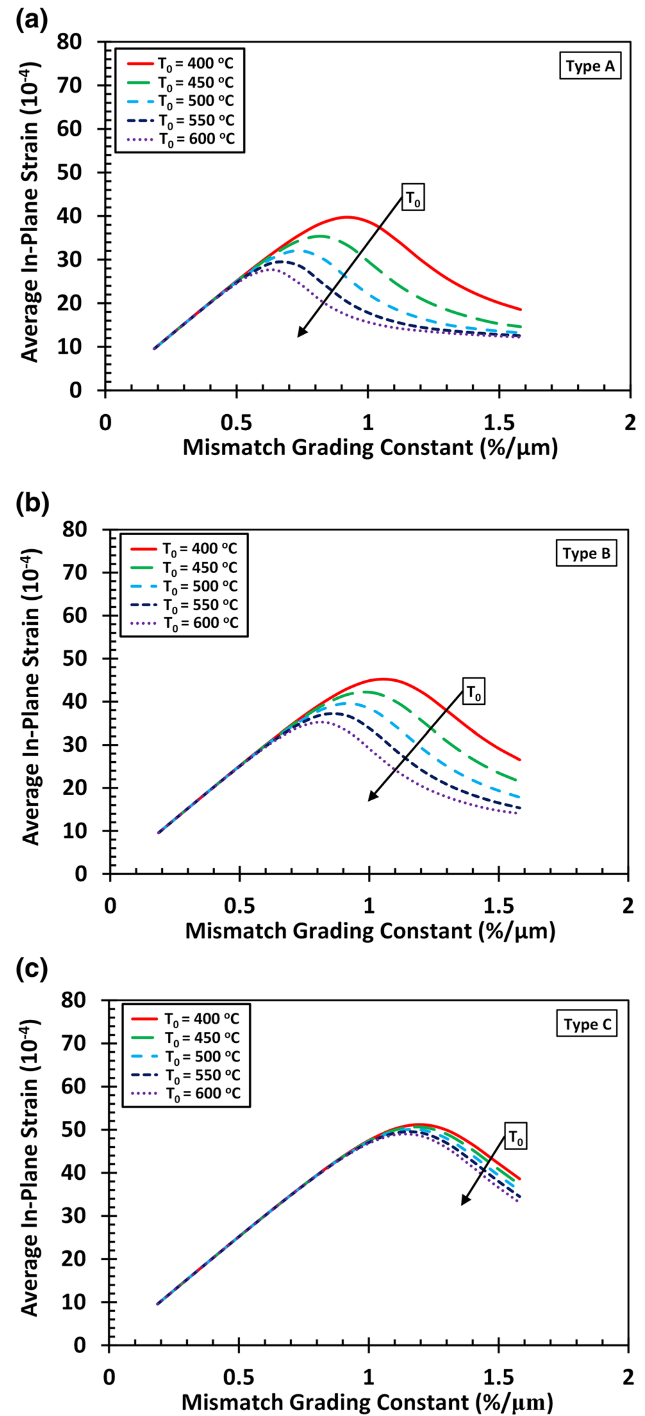

Fig. 3. Average kinetically limited in-plane strain as function of grading constant C_f with initial temperature as parameter for type (a) A, (b) B, and (c) C structures. The initial temperature T_0 is varied from 400°C to 600°C in steps of 50°C, and the final temperature T_F is fixed at 300°C.

structures, 95% relaxation occurs at $C_f \approx 1.2\%/\mu$m and $C_f \approx 1.9\%/\mu$m, respectively. It should also be noted that use of lower thermal budget results in reduced curve separation. As an example, for type C structures with grading constant of 1.58%/μm, changing the initial temperature from 400°C to 600°C results in a ~10% difference in average strain value.

Figure 4a–c displays the variation of the surface strain relaxation (in percent) with the lattice mismatch gradient, with initial temperature as a parameter, for the three types of structure. The results in Fig. 4a–c reinforce three key details discussed in the previous paragraph: First, the surface strain relaxation percentage is monotonically increasing with higher grading constant. Second, for given grading constant, structures with higher thermal budget (i.e., type A structures or with higher initial growth temperature) exhibit higher relaxation percentage of the surface strain. Third, the surface relaxation percentage saturates at about ~80% for the structures studied here. From a fabrication point of view, the surface strain is important in device design of multilayered heterostructures, because it allows flexibility to control the strain at the top of the buffer layer. The results in Figs. 3 and 4 show that, for given grading constant, the surface and average strain can be tightly controlled by optimizing the temperature grading profile. Furthermore, the results in Fig. 4 indicate that, for given temperature profile, it may be possible to control the onset of lattice relaxation (and therefore the surface strain), the rate at which strain relaxation occurs for increasing grading constant, and the maximum relaxation percentage attainable. Moreover, for the sake of comparison, we also calculated the strain relaxation in otherwise identical samples grown at constant temperature of 300°C or 600°C. For the heterostructures studied in this work, such growth at constant temperature of 300°C or 600°C yielded lower and upper bounds on the lattice relaxation, respectively. A key result from Fig. 4 is that structures with the greatest thermal budget will exhibit the highest relaxation percentage. Therefore, we can conclude that structures grown at constant temperature of 600°C will exhibit the highest relaxation percentage (lowest surface in-plane strain value), whereas structures grown at a constant 300°C will exhibit the lowest relaxation percentage (highest surface in-plane strain); For example, in a heterostructure with grading coefficient of 1.205%/μm, use of a type A temperature grading profile with T_0 = 600°C and T_F = 300°C resulted in surface strain relaxation of 61.2%, whereas structures of type B and C yielded 54.5% and 18.9%, respectively. Furthermore, structures grown at constant temperature of 300°C or 600°C exhibited a surface relaxation percentage of 12.55% and 73.11%, respectively. In the specific case of ZnSSe, it is desirable to use a low ending growth temperature to optimize the optical properties of the material. Therefore, temperature grading allows us the flexibility to adjust the strain relaxation and in-plane strain while keeping the ending growth temperature fixed. Also, in a more general sense, temperature grading is of interest

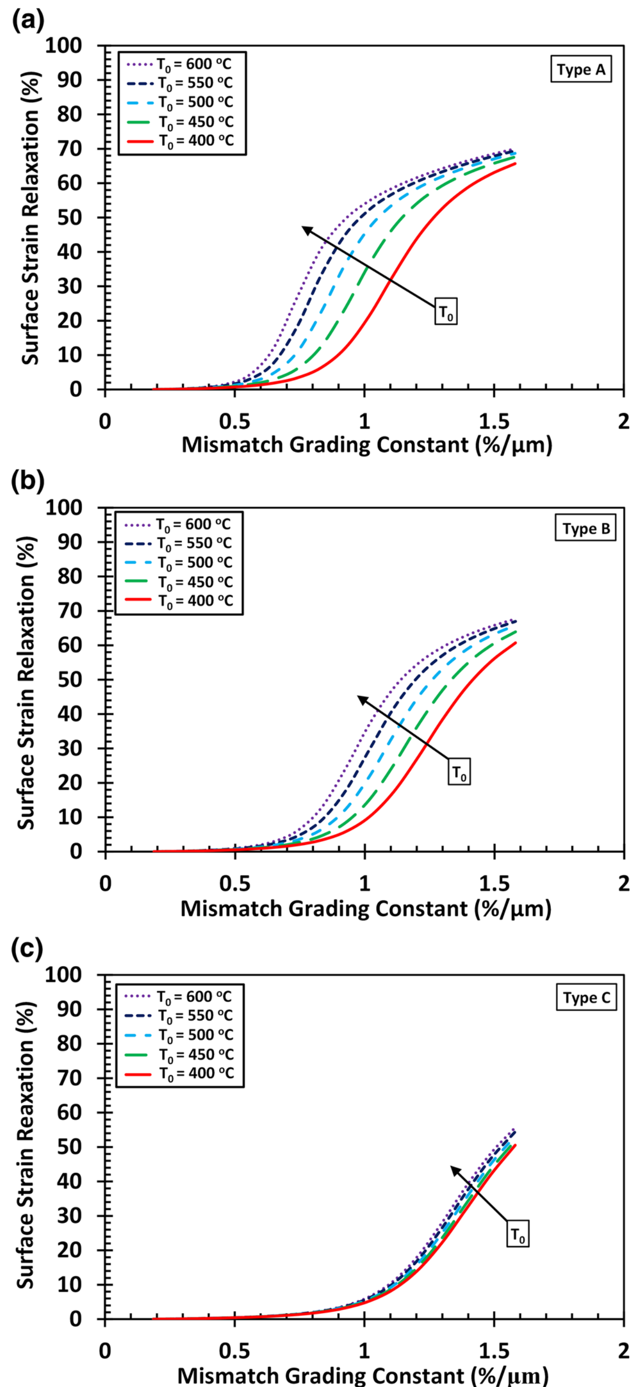

Fig. 4. Surface strain relaxation percentage as function of grading constant C_f with initial temperature as parameter for type (a) A, (b) B, and (c) C structures. The initial temperature T_0 is varied from 400 to 600°C in steps of 50°C, and the final temperature T_F is fixed at 300°C.

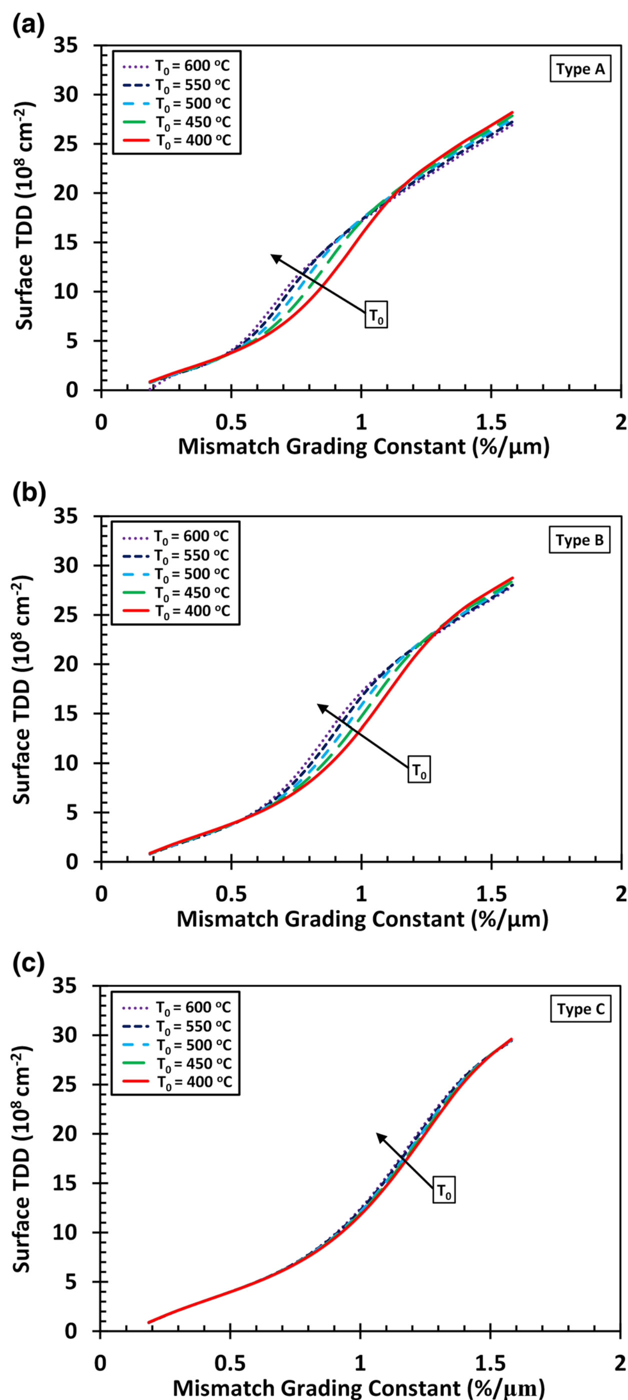

Fig. 5. Surface threading dislocation density as function of grading constant C_f with initial temperature as a parameter for type (a) A, (b) B, and (c) C structures. The initial temperature T_0 is varied from 400 to 600°C in steps of 50°C, and the final temperature T_F is fixed at 300°C.

because, in principle, it could allow depth grading of the average misfit dislocation length, thereby controlling the threading dislocation behavior.

Figure 5a–c show the surface threading density versus layer thickness with starting growth temperature as a parameter for type A (Fig. 5a), B (Fig. 5b), and C (Fig. 5c) structures. The dislocation behavior in the structures studied here is slightly more complex in comparison with the kinetically limited in-plane strain, but the results in Fig. 5 indicate a monotonically increasing dislocation density with increasing grading constant. Each type of buffer structure exhibits three regimes of threading dislocation behavior: In the first regime, there exists an initial and sluggish build-up of threading dislocations associated with layers which are in the early stages of lattice relaxation. At relatively low grading coefficient, the dislocation density for a given structure type is independent of the initial temperature condition. Based on the results in Fig. 2, structures which exhibit low relaxation rates and therefore higher in-plane strain are more favorable for sweeping out threading arms. The second regime corresponds to a rapid relaxation phase, whereby threading dislocations are introduced at a more rapid rate to relax the excess mismatch strain. Furthermore, structures with higher initial growth temperature contain higher density of surface dislocations. However, in structures with lower thermal budget, we see reduced curve separation and therefore temperature independence of dislocation density. In addition, for higher grading constants, the surface threading dislocation density is comparable among the three structure types. Also, for these structures, there exists a grading constant beyond which the threading dislocation density is lower for higher thermal budget. This phenomenon can be explained based on the fact that higher thermal budget leads to structures with higher dislocation density, which can enable greater reduction in the dislocation density due to thermally activated glide. However, it should be noted that the surface strain contained in these structures plays an important role in the control of threading dislocations.

CONCLUSIONS

We investigated the evolution of kinetically limited lattice relaxation by dislocation generation in ZnS_ySe_{1-y}/GaAs (001) heterostructures involving a combination of compositionally and temperature-graded buffer layers. The results lead to two main findings: First, structures grown at higher average temperature (with greater thermal budget) or with steeper compositional gradient show greater extent of relaxation and reduced residual in-plane strain; Second, structures with higher in-plane strain contain lower threading dislocation density, but at higher grading constant, it may be possible to tailor the temperature profile such that relatively low threading dislocation densities may be attainable. Extension of this work could include structures exhibiting epilayer thickness variation.

REFERENCES

1. J. Tersoff, *Appl. Phys. Lett.* 62, 693 (1993).

2. J. Tersoff, *Appl. Phys. Lett.* 64, 2748 (1994).
3. E.A. Fitzgerald, Y.-H. Xie, D. Monroe, P.J. Silverman, J.M. Kuo, A.R. Kortan, F.A. Thiel, and B.W. Weir, *J. Vac. Sci. Technol. B* 10, 1807 (1992).
4. A. Sacedon, F. Gonzalez-Sanz, E. Calleja, E. Munoz, S.I. Molina, F.J. Pacheco, D. Araujo, R. Garcia, M. Lourenco, Z. Yang, P. Kidd, and D. Dunstan, *Appl. Phys. Lett.* 66, 3334 (1995).
5. S. Takeuchi, Y. Shimura, O. Nakatsuka, S. Zaima, M. Ogawa, and A. Sakai, *Appl. Phys. Lett.* 92, 231916 (2008).
6. J.I. Chyi, J.L. Shieh, J.W. Pan, and R.M. Lin, *J. Appl. Phys.* 79, 8367 (1996).
7. E.F. Chor and C.J. Peng, *Electron. Lett.* 32, 1409 (1996).
8. H. Choi, Y. Jeong, J. Cho, and M.H. Jeon, *J. Cryst. Growth* 311, 1091 (2009).
9. B. Bertoli, D. Sidoti, S. Xhurxhi, T. Kujofsa, S. Cheruku, J.P. Correa, P.B. Rago, E.N. Suarez, J.E. Ayers, and F.C. Jain, *J. Appl. Phys.* 108, 113525 (2010).
10. S. Xhurxhi, F. Obst, D. Sidoti, B. Bertoli, T. Kujofsa, S. Cheruku, J.P. Correa, P.B. Rago, E.N. Suarez, F.C. Jain, and J.E. Ayers, *J. Electron. Mater.* 40, 2348 (2011).
11. T. Kujofsa, A. Antony, S. Xhurxhi, F. Obst, D. Sidoti, B. Bertoli, S. Cheruku, J.P. Correa, P.B. Rago, E.N. Suarez, F.C. Jain, and J.E. Ayers, *J. Electron. Mater.* 42, 3408 (2013).
12. D.E. Grider, S.E. Swirhun, D.H. Narum, A.I. Akinwande, T.E. Nohava, W.R. Stuart, and P. Joslyn, *J. Vac. Sci. Technol. B* 8, 301–304 (1990).
13. K. Inoue, J.C. Harmand, and T. Matsuno, *J. Cryst. Growth* 111, 313–317 (1991).
14. L. Shen, H.H. Wieder, and W.S.C. Chang, *Mater. Res. Soc. Symp.* 379, 297–301 (1997).
15. A. Wakita, H. Rohden, V. Robbins, N. Mll, C.-Y. Su, A. Nagy, and D. Basile, *Jpn. J. Appl. Phys.* 38, 1186–1189 (1999).
16. X.Z. Shang, S.D. Wu, C. Liu, W.X. Wang, L.W. Guo, and Q. Huang, *J. Phys. D* 39, 1800–1804 (2006).
17. B. Lee, J.H. Baek, J.H. Lee, S.W. Choi, S.D. Jung, W.S. Han, and E.H. Lee, *Appl. Phys. Lett.* 68, 2973–2975 (1996).
18. I. Tangring, H.Q. Ni, B.P. Wu, D.H. Wu, Y.H. Xiong, S.S. Huang, Z.C. Niu, S.M. Wang, Z.H. Lai, and A. Larsson, *Appl. Phys. Lett.* 91, 221101 (2007).
19. J.-F. He, H.-L. Wang, X.-J. Shang, M.-F. Li, Y. Zhu, L.-J. Wang, Y. Yu, H.-Q. Ni, Y.-Q. Xu, and Z.-C. Niu, *J. Phys. D* 44, 335102 (2011).
20. T. Kujofsa and J.E. Ayers, *J. Electron. Mater.* 44, 3030 (2015).
21. B.W. Dodson and J.Y. Tsao, *Appl. Phys. Lett.* 51, 1325 (1987).
22. B.W. Dodson and J.Y. Tsao, *Appl. Phys. Lett.* 52, 852 (1988).
23. M. Tachikawa and M. Yamaguchi, *Appl. Phys. Lett.* 56, 484 (1990).
24. B. Bertoli, E.N. Suarez, J.E. Ayers, and F.C. Jain, *J. Appl. Phys.* 106, 073519 (2009).
25. T. Kujofsa, W. Yu, S. Cheruku, B. Outlaw, F. Obst, D. Sidoti, B. Bertoli, P.B. Rago, E.N. Suarez, F.C. Jain, and J.E. Ayers, *J. Electron. Mater.* 41, 2993 (2012).
26. T. Kujofsa, S. Cheruku, W. Yu, B. Outlaw, S. Xhurxhi, F. Obst, D. Sidoti, B. Bertoli, P.B. Rago, E.N. Suarez, F.C. Jain, and J.E. Ayers, *J. Electron. Mater.* 42, 2764 (2013).
27. J.W. Matthews, *J. Vac. Sci. Technol.* 12, 126 (1975).
28. J.W. Matthews and A.E. Blakeslee, *J. Cryst. Growth* 27, 118 (1974).
29. A.E. Romanov, W. Pompe, G.E. Beltz, and J.S. Speck, *Appl. Phys. Lett.* 69, 3342 (1996).